Nanoscale

Critical Length Scales and Strain Localization Govern the Mechanical Performance of Multi-layer Graphene Assemblies

Journal:	*Nanoscale*
Manuscript ID	NR-COM-11-2015-008488.R1
Article Type:	Communication
Date Submitted by the Author:	08-Jan-2016
Complete List of Authors:	Xia, Wenjie; Northwestern University, Civil and Environmental Engineering Ruiz, Luis; Northwestern University, Theoretical and Applied Mechanics Pugno, Nicola; University of Trento, Civil, Environmental and Mechanical Engineering; Queen Mary University of London, School of Engineering and Materials Sciences Keten, Sinan; Northwestern University, Mechanical Engineering

Critical Length Scales and Strain Localization Govern the Mechanical Performance of Multi-layer Graphene Assemblies

Wenjie Xia[1], Luis Ruiz[2], Nicola M. Pugno[3,4,5], Sinan Keten[1,2*]

[1]Department of Civil & Environmental Engineering, Northwestern University, 2145 Sheridan Road, Evanston, IL 60208, United States

[2]Department of Mechanical Engineering, Northwestern University, 2145 Sheridan Road, Evanston, IL 60208, United States

[3]Department of Civil, Environmental and Mechanical Engineering, University of Trento, Via Mesiano 77, 38123 Trento, Italy

[4]Center for Materials and microsystems, Fondazione Bruno Kessler, Via Sommarive 18, 38123 Trento, Italy

[5]School of Engineering and Materials Science, Queen Mary University of London, Mile End Road, London E1 4NS, United Kingdom

* Corresponding Author: Dept. of Civil & Environmental Engineering and Dept. of Mechanical Engineering, Northwestern University, 2145 Sheridan Road, Evanston, IL 60208. Tel: 847-491-5282, Email: s-keten@northwestern.edu

Abstract

Multi-layer graphene assemblies (MLGs) with a staggered architecture exhibit high toughness and failure strain that surpass those of the constituent single sheets. However, how the architectural parameters such as sheet overlap length affect these mechanical properties remains

unknown due in part to limitations of mechanical continuum models. By exploring the mechanics of MLG assemblies under tensile deformation using our established coarse-grained molecular modeling framework, we identify three different critical interlayer overlap lengths controlling the strength, plastic stress, and toughness of MLGs, respectively. The shortest critical length scale L_c^s governs the strength of the assembly as predicted by the shear-lag model. The intermediate critical length L_c^p is associated to a dynamic frictional process that governs the strain localization propensity of the assembly, and hence the failure strain. The largest critical length scale L_c^T corresponds to the overlap length necessary to achieve 90% of the maximum theoretical toughness of the material. Our analyses provide general guidelines for tuning constitutive properties and toughness of multilayer 2D nanomaterials using elasticity, interlayer interaction energy and geometry as molecular design parameters.

ARTICLE

Graphene, one of the strongest materials known,[1-3] is particularly suited for advanced structural and mechanical applications.[4, 5] In practice, its range of application remains limited due to the difficulty of harnessing the mechanical properties at larger length scales than those limited by the processing and synthesis of individual graphene sheets (in the order of nanometers to a few micrometers). In addition, its low extensibility and brittle failure behavior further restricts the usage in electronics, energy storage devices, and other applications where toughness and ductility are critical.

Drawing inspiration from biological architectures such as nacre, one possible way to simultaneously increase its extensibility and harness the properties of graphene in a scalable manner is to stack multiple sheets in a staggered fashion forming a so-called multi-layer

graphene assembly (MLG).[6-12] In materials with multi-layer staggered architecture the tensile load is transferred through shear at the interfaces and the deformation occurs by relative sliding between the sheets in different layers.[13] For small deformations, where sheet and interface behave linearly elastic to a good approximation, the continuum shear-lag model can be used to adequately predict the mechanical properties.[14-17] However, as the deformation increases and more complex deformational mechanisms, such as strain localization, are activated, the shear-lag model breaks down. Understanding how architectural parameters, in particular the overlap length between sheets in different layers, impact the mechanical behavior of the assembly is of critical importance for the rational design of optimal MLGs and other engineered materials with analogous architecture. Here, we use coarse-grained molecular dynamics (CG-MD) of MLGs under uniaxial tensile strain to identify the critical overlap length scales that control the strength, toughness and failure strain.

The CG molecular model of graphene used here (Fig. 1(a)) has been shown to accurately reproduce the elastic and fracture properties of single crystal graphene, as well as its interlayer shear behavior.[18] Details of the CG force-field can be found in the original publication[18] but have also been included in the SI, together with a detailed presentation of the simulation parameters and protocols used in this work. We have simulated multiple MLG systems with varying number of layers (n_l = 2, 3, 5, and 10) and one sheet per layer (n_s = 1), which constitute a representative volume element (RVE) (Fig. 1(b)). The simulated MLGs in the RVE have overlap lengths L_o ranging from ~ 3 to 780 nm. The sheet's width is set to be 6.4 nm for all the cases and our preliminary results indicate that the width does not affect our findings. Each graphene sheet in the assembly is a single crystal without defects. We do not consider grain boundary effects as the typical grain size of graphene (~10 μm) is much larger than the sizes of our system.[19] To verify

that our findings are applicable to multiple sheets per layer, we also perform simulations for the n_s= 3 case. The results have been included in the Supporting Information (SI) and do not alter any of the conclusions presented. It is worth noting that the bonds of the CG model are breakable and that no further constraints, other than the imposed uniaxial strain, are used, i.e., we do not impose any a-priori failure or deformational mechanisms on the system.

The typical stress-strain response of MLGs exhibits a short linear elastic regime that ends with a sudden drop in the stress. A plastic regime that ends in a rapid decay of the stress until failure follows the stress drop (Fig. 1(c)). At the microscopic level, the fundamental deformational process of interlayer sliding is not continuum and consists of discrete transitions between commensurate stacking configurations of graphene sheets in neighboring layers (i.e. stick-slip mechanism). The elastic regime in this microscopic picture corresponds to the deformational period before the system undergoes the first slip event, which occurs within the range from ~1% to 4% strain depending on L_o for the all the cases studied (inset of Fig. 1(c)). For small deformations, the van der Waals-governed interfaces and the sheets behave linearly elastic, and the tensile stress of MLGs is resulted from the static friction between layers. Under these conditions, the Young's modulus and the maximum stress σ_m, which we also refer as the tensile strength here, can be predicted by the continuum shear-lag model:[14, 15]

$$\sigma_m = \frac{\sinh(L_o / l)\gamma_s^{cr} E_g h}{2(1+\cosh(L_o / l))l} \quad (1)$$

where $l = \sqrt{\frac{E_g h^2}{4G}}$ ($\approx$ 5.2 nm) is a parameter that represents the length scale over which most of the stress is transferred in the interface, E_g(~ 950 GPa) is the Young's modulus of graphene, G(~1 GPa) is the shear modulus of the interface, h(= 3.35 Å) is the equilibrium interlayer distance between the two layers, and γ_s^{cr}(~0.35) is the critical interlayer shear strain. The values

of these fundamental parameters are set by the properties of the CG model.[18] The prediction of the MLG strength by the shear-lag model as a function of L_o is in very good agreement with the simulation results (Fig. 1(d)). If we define the critical length scale governing the strength of MLGs as the L_o at which 90% of the maximum strength is achieved, we obtain $L_c^s \sim 17$ nm, which is consistent with previous theoretical calculations that predicted $L_c^s \sim 3\ l$ for an analogous system.[17] Although the maximum strength of MLGs (~10 GPa) is an order of magnitude lower than that of monocrystalline graphene (~100 GPa),[1] its strength still surpasses most of structural engineered materials.

At the end of the elastic regime we observe a sudden drop in stress. We associate this drop to the transition from a static (before the first slip event) to a dynamic frictional situation [20, 21] (referred here as the plastic regime because the deformations are irreversible). This drop after the peak stress could originate from the irregular stress distributions within the sheet, which will not strictly follow the shear-lag prediction. The plastic stress, σ_p, is defined as the average stress in the plateau plastic regime, which is indicated by the horizontal dashed lines in Fig 1(c). Interestingly, the dependence of the post-peak plastic stress σ_p on L_o reveals that shear-lag scaling still holds (Fig. 1(d)). In fact, the trend can be quantitatively captured by Eq. (1) if l (~ 16.3 nm) and γ_{cr} (~ 0.67) are used as fitting parameters. This resulting weaker interface (i.e. softer and more ductile) in the plastic regime compared to the interface properties at small deformations is compatible with the static-to-dynamic frictional transition proposition. Similar to the critical length scale identified for strength, we can define a second critical length scale associated with the saturation of the plastic stress to a near maximum value around $L_c^p \approx 50$ nm.

The physical meaning of L_c^P becomes clear when looking at the mechanical response of a single interface. Fig. 2(a) illustrates the bilayer model with a single interface used to characterize

the constitutive force-displacement (f-u) response. To simplify our analysis, we apply the bilinear curve to characterize the f-u response (Fig. 2(b)). It can be observed that the nearly constant force regime lasts until the displacement u reaches ~ $(L_o - L_c^P)$, after which the force decays approximately linearly up to failure by complete loss of overlap between the sheets. This analysis suggests that L_c^P is the critical overlap length after which the shear force at the interface does not depend on the overlap length. This observation can also be inferred from the shear-lag theory in which the strength σ_s and plastic stress σ_p are nearly independent of L_o as L_o beyond L_c^s and L_c^P, respectively.

To be able to generalize these findings to other 2D materials, we need to understand the dependence of L_c^P on the constituent material properties, in particular the Young's modulus of and interlayer adhesion energy. According to the shear-lag model,[22] the critical length scale at which the tensile strength starts to saturate follows the scaling, $L_c^s \sim \sqrt{\frac{E_g}{G}}$. In the stick-slip microscopic deformational mechanism the shear rigidity depends linearly on the adhesion energy γ between the two sheets ($G \sim \gamma$). Therefore, from a theoretical standpoint, we expect L_c^p to follow a similar scaling, $L_c^p \sim \sqrt{\frac{E}{\gamma}}$. In fact, we find that the best fits to the simulation results $L_c^P \sim (E/E_g)^{0.41}$ and $L_c^P \sim 1/(\gamma/\gamma_g)^{0.52}$ (Fig. 3(a) and 3(b)), are in close agreement with the shear-lag exponent of 0.5. Although L_c^p may also depend on other factors, such as the pulling velocity as in the case of atomic friction,[21, 23] we expect the scaling on constituent material properties to hold at a given rate.

Visualization of the simulation trajectories reveals that the deformation is uniformly distributed over all of the interfaces up to a certain point (the intermediate state), after which the strain localizes in a certain region along the length of the MLG (Fig. 4(a) and Movie S1). The

system ends up failing by deoverlapping in the region where the strain localizes. The deformation process identified from our simulations is schematically illustrated in Fig. 4(b). We characterize the intermediate state or equivalently the onset of localization by the displacement of each interface u_{int} at that moment. After the intermediate the strain localizes only on one side that keeps deoverlapping until failure. Using simple geometric arguments, one can show that if localization occurs irreversibly at u_{int} the failure strain ε_f is directly related to u_{int} via:

$$\varepsilon_f = \frac{u_{\text{int}}}{2L_o} + \frac{1}{2} \tag{2}$$

or more generally for n_s sheets per layer,

$$\varepsilon_f = \frac{(2n_s - 1)u_{\text{int}}}{2n_s L_o} + \frac{1}{2n_s} \tag{3}$$

In order to predict the failure strain of the MLG, we need to know when strain localization occurs, or equivalently the value of u_{int}. Shearing of an interface proceeds through a series of slips between equilibrium states where the lattices are in commensurate positions. Thus, we can think of interlayer sliding as a series of thermally activated jumps over energy barriers.[24, 25] and use a kinetic model based on Bell's theory [26-28] to describe the shear behavior of each interface. The lifetime, τ, of a single jump under an applied force is given by $\tau = \exp\left(\frac{E_b - x_b f}{k_B T}\right)/\omega_0$, where ω_0 ($\sim 1\times10^{13}$ 1/s) is the vibrational frequency of the interface in the energy well [26], $k_B T$ is the thermal energy, and x_b is the distance from equilibrium to the transition state, which depends on the lattice spacing. The probability P_{over} of overcoming an energy barrier and advancing the system to the next equilibrium state (i.e. slipping) within a time interval Δt can therefore be approximated by: $P_{over} = 1 - \exp\left(-\frac{\Delta t}{\tau}\right)$. Using this theoretical scheme, we can numerically simulate the deformation of two interfaces in mechanical equilibrium and measure u_{int}, which

would correspond to the displacement at which one of the interfaces gets trapped in a local minimum while the other keeps sliding under the applied force. A detailed description of this kinetic model is given in the SI. The results of this model reveal that strain localization always initiates when the displacement is $u_{int} = L_o - L_c^p$, for $L_o > L_c^p$. This finding suggests that L_c^p is a critical length also associated to strain localization, and hence failure strain. Substituting $u_{int} = L_o - L_c^p$ into Eq. (2), ε_f can be directly expressed as:

$$\varepsilon_f = 1 - \frac{L_c^p}{2L_o} \tag{4}$$

This equation accurately captures the ε_f obtained from the kinetic model analysis (Fig. 4(c)). When $L_o < L_c^p$, the kinetic model predicts that localization initiates from the start, which leads to $\varepsilon_f \sim 0.5$. It is worth noting that the minimum and maximum theoretical failure strain in this system ($n_s = 1$) is 0.5 and 1 respectively. The predictions of the kinetic model agree with what is observed in the CG-MD simulations for $L_o > L_c^p$ (Fig. 4(d)), suggesting that the origin of the strain localization is kinetic trapping of one of the interfaces in a local minimum. For $L_o < L_c^p$, the CG-MD simulations show slightly greater failure strains than the kinetic model predictions, which we attribute to the fact that at a finite rate and short L_o, some homogeneous deformation can still carry on before strain localization occurs. It should be noted that changing the x_b of the CG model to the value of atomistic graphene will not change the kinetic model predictions.

Once we are able to theoretically predict the plastic stress and the failure strain of MLGs, we can attempt to predict the toughness of the system, or equivalently its energy dissipation capacity, defined as the area under the stress-strain curve. If we follow the definition of toughness and simplify the stress-strain response as a constant plateau at σ_p followed by a linear decay after strain localization, T can be directly approximated by a simple expression:

$$T = \int_0^{\varepsilon_f} \sigma d\varepsilon = \sigma_p (1 - \frac{L_c^p}{L_o}) + \frac{\sigma_p}{4n_s} \frac{L_c^p}{L_o} \quad (5)$$

The quantitative agreement between this relationship and the toughness from the simulations is remarkable considering the simplicity of the model (Fig. 5(a)). Notably, Eq. (5) implies that the toughness of MLG saturates at large L_o. Defining the critical length as before following the 90% criteria, we get $L_c^T \approx$400 nm or ~$8L_c^p$ for $n_s = 1$. Further increase in L_o beyond this critical length will not enhance the toughness significantly. This critical overlap length L_c^T is an extremely relevant design guideline for the design of tough MLG papers. Our simulations show that the theoretical maximum toughness (~7×10^3 MJ/m^3) or specific energy dissipation (E_p^*~3 MJ/kg) that can be achieved by the MLG is roughly an order of magnitude higher comparing to other engineering materials, such as steel or Kevlar armor.[19, 29, 30] Our simulations also suggest that the theoretical maximum toughness values are much higher than those recently measured by supersonic ballistic experiments on MLGs (E_p^*~1.5 MJ/kg).[19]

It is important to notice that the energy of the intralayer interactions (i.e. interactions between different sheets in the same layer) is negligible compared to the surface energy between sheets in different layers. This is because within each layer, the side-by-side interaction energy of the graphene sheets is much smaller than the strength of the covalent bonds within each sheet, so its contribution to features such as modulus and strength are negligible. Most of the load transfer occurs through shear transfer across layers rather than through serial force transfer between sheets in the same layer. Accordingly we have not included these edge effects in the analysis presented above. Also, although we considered only monocrystalline graphene for our sheets, the presence of grain boundaries will most likely not change our results, as the energy to break those bonds will still be much larger than the shear barriers imposed by the weak van der Waals

interactions, maintaining the failure mode by deoverlapping unchanged. These assumptions will need to be revisited if the system under study includes cross-links that strengthen the intralayer interactions or the interfaces.

Our findings provide several strategies for improving toughness. First, given that L_c^T is directly related to L_c^p, the failure strain and toughness can be controlled by tuning the stiffness E of the constituent sheets and the interfacial adhesion energy γ between the sheets by functionalizing the surface. The prediction of L_c^T as a function of E and γ is shown in Fig. 5(b). There are various pathways through which these material properties could be tailored. For example, by oxidizing the carbon atoms at different functionalization levels (the fraction of oxidized carbon atoms), forming the so-called graphene oxide (GO) paper, the enhanced interfacial adhesion energy and reduced modulus compared to pristine graphene can be utilized to design these length scale parameters and thus materials toughness.[4, 31] Second, the interlayer shear response of graphene, such as shear modulus, interaction energy, and frictional force, depends on the stacking orientation due to the hexagonal lattice feature,[18, 32, 33] and thus it would be expected that L_c^p and L_c^T also varies for different stacking order (e.g. Bernal vs. turbostratic). The scaling of L_c^p relations for dependence on factors such as critical shear strain and adhesion energy can be readily used to predict L_c^T for different stacking orientations. Such predictions may enable the design of tougher protection materials, since recent projectile penetration experiments have already shown multilayer graphene to be excellent for this purpose due to its superior energy absorption capacity.[19] Our findings on mechanical behaviors of MLG with staggered architecture can be applied to design materials with dramatically enhanced toughness and energy adsorption. Moreover, our results of the size-dependent mechanical response and failure mechanism of MLG can be adapted to other 2D materials whose interfacial properties are governed by vdW

interactions as well, such as phosphorene, MoS_2 and hBN.[34-37] For instance, for the case of phosphorene which has a rougher potential energy landscape and a lower sheet stiffness compared to graphene, its L_c^T of a multilayer system will be smaller than that of graphene based on our predictions as shown in Fig. 5(b). Future work on theoretical description of plastic stress associated with the dynamic friction process will be a key to quantitatively predicting the mechanical responses of multi-layer assemblies of 2D nanomaterials at large deformation regime.

Conclusions

In summary, we have performed CG-MD simulations to provide unprecedented quantitative understanding of the dependence of the mechanical properties of MLG on interlayer overlap length L_o, including the elusive large deformation and failure regimes where continuum models often break down. We have developed analytical expressions for a hierarchy of critical overlap lengths that govern the strength (L_c^S~17 nm), failure strain and plastic stress (L_c^P~50 nm), and the toughness (L_c^T~400 nm) of MLGs. Particularly interesting, we found that the toughness of MLGs, and therefore its ability to dissipate energy, does not significantly increase with overlap length for very large L_o beyond ~L_c^T. In fact, 90% of the maximum theoretical toughness can already be achieved for overlap lengths ~L_c^T, which can be considered as an extremely important design parameter to design tough multilayer graphene systems. More importantly, we have elucidated the functional dependence of these critical length scales with the mechanical properties of the constituent materials, thus providing transferrable guidelines to assemblies with similar multi-layered staggered architectures based on 2D materials with different interfacial or elastic properties, such as phosphorene, MoS_2 and hBN.

Acknowledgements

The work is funded by the National Science Foundation (DMREF award CMMI-1235480). The authors acknowledge the support from the Departments of Civil and Environmental Engineering and Mechanical Engineering at Northwestern University, as well as the Northwestern University High Performance Computing Center for a supercomputing grant. We thank our collaborators Horacio Espinosa, SonBinh T. Nguyen and Jeff Paci for fruitful discussions on the mechanics and computational modeling of multi-layered graphene.

References

1. C. Lee, X. D. Wei, J. W. Kysar and J. Hone, *Science*, 2008, **321**, 385-388.
2. C. Lee, X. D. Wei, Q. Y. Li, R. Carpick, J. W. Kysar and J. Hone, *Phys. Status Solidi B*, 2009, **246**, 2562-2567.
3. F. Liu, P. M. Ming and J. Li, *Physical Review B*, 2007, **76**.
4. Y. W. Zhu, S. Murali, W. W. Cai, X. S. Li, J. W. Suk, J. R. Potts and R. S. Ruoff, *Adv. Mater.*, 2010, **22**, 3906-3924.
5. R. J. Young, I. A. Kinloch, L. Gong and K. S. Novoselov, *Compos. Sci. Technol.*, 2012, **72**, 1459-1476.
6. M. J. Buehler, *Proc. Natl.l Acad. Sci. USA*, 2006, **103**, 12285-12290.
7. H. D. Espinosa, J. E. Rim, F. Barthelat and M. J. Buehler, *Prog. Mater. Sci.*, 2009, **54**, 1059-1100.
8. P. Egan, R. Sinko, P. R. LeDuc and S. Keten, *Nat. Commun.*, 2015, **6**.
9. H. Chen, M. B. Muller, K. J. Gilmore, G. G. Wallace and D. Li, *Adv. Mater.*, 2008, **20**, 3557-3561.
10. O. C. Compton and S. T. Nguyen, *Small*, 2010, **6**, 711-723.
11. D. Li, M. B. Muller, S. Gilje, R. B. Kaner and G. G. Wallace, *Nat. Nanotechnol.*, 2008, **3**, 101-105.
12. C. Shao and S. Keten, *Sci. Rep.*, 2015, **5**, 16452.
13. B. H. Ji and H. J. Gao, *Annu. Rev. Mater. Res.*, 2010, **40**, 77-100.
14. H. L. Cox, *Brit. J. Appl. Phys.*, 1952, **3**, 72-79.
15. B. Chen, P. D. Wu and H. Gao, *Compos. Sci. Technol.*, 2009, **69**, 1160-1164.
16. X. D. Wei, M. Naraghi and H. D. Espinosa, *ACS Nano*, 2012, **6**, 2333-2344.
17. Y. Liu, B. Xie, Z. Zhang, Q. Zheng and Z. Xu, *J. Mech. Phys. Solids*, 2012, **60**, 591-605.

18. L. Ruiz, W. J. Xia, Z. X. Meng and S. Keten, *Carbon*, 2015, **82**, 103-115.
19. J.-H. Lee, P. E. Loya, J. Lou and E. L. Thomas, *Science*, 2014, **346**, 1092-1096.
20. B. N. Persson, *Sliding friction: physical principles and applications*, Springer Science & Business Media, 2000.
21. H. Hölscher, A. Schirmeisen and U. D. Schwarz, *Phil. Trans. R. Soc. A*, 2008, **366,** 1383-1404.
22. N. Pugno, Q. Yin, X. Shi and R. Capozza, *Meccanica*, 2013, **48**, 1845-1851.
23. O. Zworner, H. Holscher, U. D. Schwarz and R. Wiesendanger, *Appl. Phys. A Mater. Sci.*, 1998, **66**, S263-S267.
24. G. A. Tomlinson, *Philos. Mag.*, 1929, **7**, 905-939.
25. L. Prandtl, *Z. angew. Math. Mech.*, 1928, **8**, 85-106.
26. G. Bell, *Science*, 1978, **200**, 618-627.
27. S. Keten and M. J. Buehler, *Phys. Rev. E*, 2008, **78**.
28. S. Keten and M. J. Buehler, *Nano Lett.*, 2008, **8**, 743-748.
29. J. Dean, C. S. Dunleavy, P. M. Brown and T. W. Clyne, *Int. J. Impact. Eng.*, 2009, **36**, 1250-1258.
30. B. L. Lee, T. F. Walsh, S. T. Won, H. M. Patts, J. W. Song and A. H. Mayer, *J. Compos. Mater.*, 2001, **35**, 1605-1633.
31. D. A. Dikin, S. Stankovich, E. J. Zimney, R. D. Piner, G. H. B. Dommett, G. Evmenenko, S. T. Nguyen and R. S. Ruoff, *Nature*, 2007, **448**, 457-460.
32. M. Dienwiebel, G. S. Verhoeven, N. Pradeep, J. W. M. Frenken, J. A. Heimberg and H. W. Zandbergen, *Phys. Rev. Lett.*, 2004, **92**.
33. I. V. Lebedeva, A. A. Knizhnik, A. M. Popov, Y. E. Lozovik and B. V. Potapkin, *Phys. Chem. Chem. Phys.*, 2011, **13**, 5687-5695.
34. Q. Wei and X. Peng, *Appl. Phys. Lett.*, 2014, **104**, 251915.
35. K. S. Novoselov, D. Jiang, F. Schedin, T. J. Booth, V. V. Khotkevich, S. V. Morozov and A. K. Geim, *Proc. Natl.l Acad. Sci. USA*, 2005, **102**, 10451-10453.
36. C. Lee, Q. Y. Li, W. Kalb, X. Z. Liu, H. Berger, R. W. Carpick and J. Hone, *Science*, 2010, **328**, 76-80.
37. A. K. Geim and I. V. Grigorieva, *Nature*, 2013, **499**, 419-425.

FIGURES

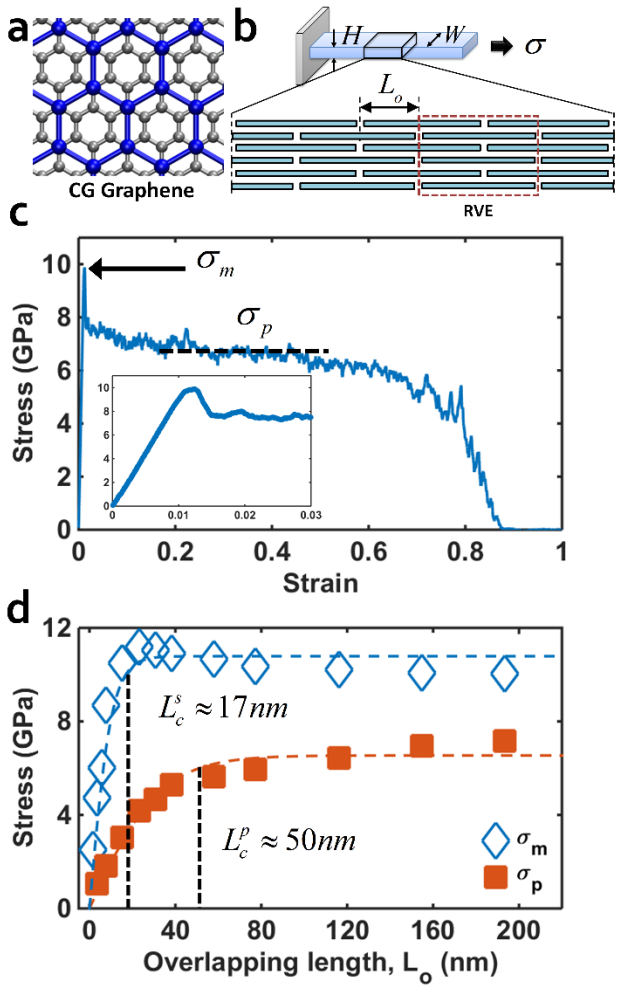

Figure 1. (a) Mapping scheme from the atomistic lattice (gray) to the coarse-grained structure (blue). **(b)** Schematic of staggered multi-layer graphene (MLG) with an overlap length of L_o. **(c)** Typical stress-strain response of MLG with L_o ~155 nm under uniaxial tension. Inset highlights the linear elastic response at small strain. **(d)** The tensile strength σ_m and plastic stress σ_p of the MLG as a function of L_o. The dashed curves are the "shear-lag" model fits to the data. L_c^s and L_c^p are the critical overlap lengths for σ_m and σ_p, respectively, beyond which the σ_m and σ_p start to saturate.

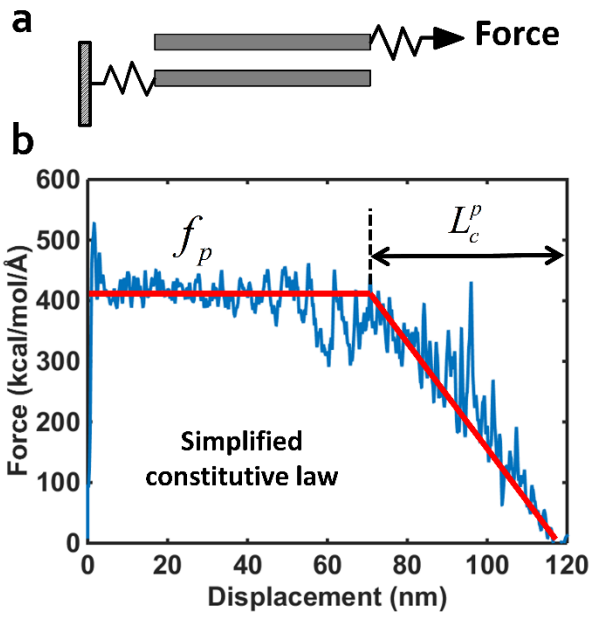

Figure 2. (a) Schematic of simplified bilayer model used to quantify the constitutive behavior of graphene with single interface. **(b)** Force-displacement (f-u) curve obtained from the pulling test. The resultant simplified constitutive law consists of a plateau force f_p regime and a linear decay regime as the remaining contact length is less than L_c^p, which is denoted by the bilinear solid lines.

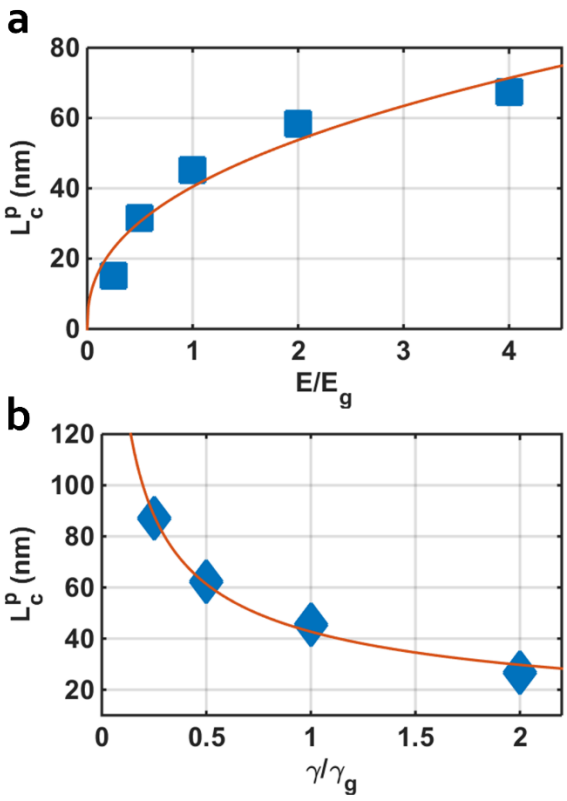

Figure 3. Dependence of the critical length L_c on **(a)** sheet stiffness E and **(b)** interlayer adhesion energy γ determined from the pulling test of the bilayer model.

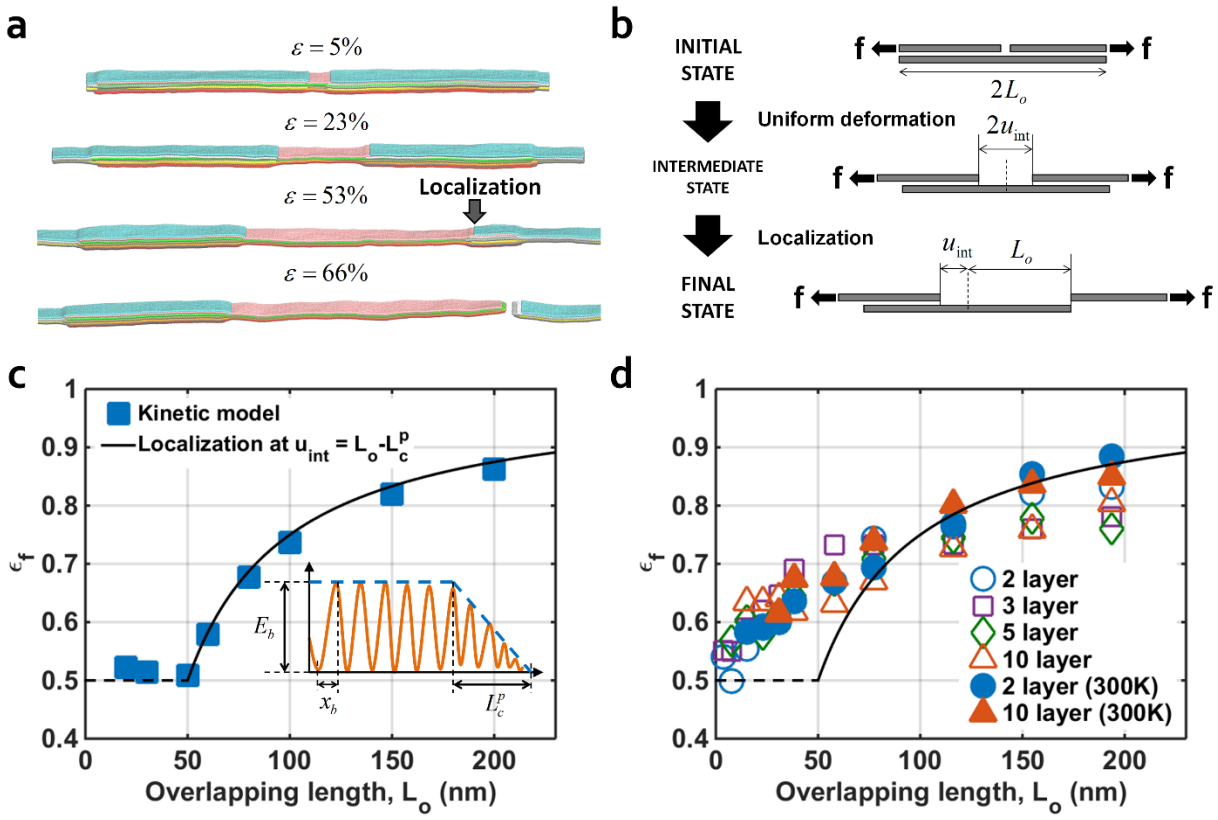

Figure 4. **(a)** MD snapshots of MLG deformation process. **(b)** Schematic of sequence of different states during the deformation process. **(c)** Kinetic model prediction and **(d)** MD simulation results of failure strain ε_f as a function of overlap length L_o. The inset of **(c)** shows the schematic of energy landscape used to predict strain localization in the simplest bilayer system. The solid curves in **(c)** and **(d)** show the scaling of n by assuming the localization occurs when the remaining contact length of each part reduces to L_c^p.

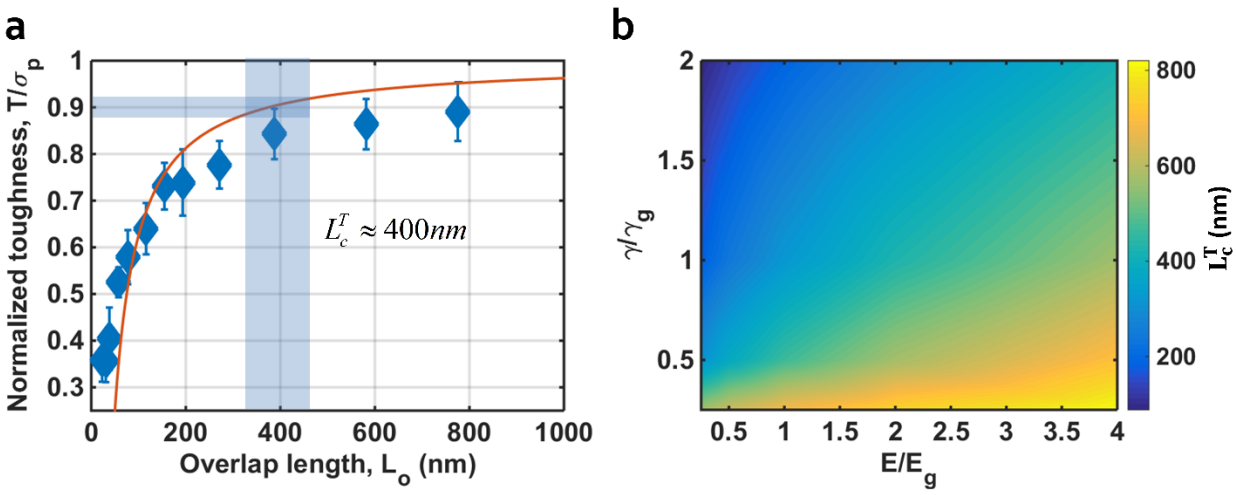

Figure 5. (a) Normalized toughness T/σ_p as a function of overlap length. The solid curve shows the prediction from Eq. (5) for n_s = 1. **(b)** The predicted critical length L_c^T for the toughness as a function of sheet stiffness E and interlayer adhesion energy γ.

For table of contents use only:

Critical Length Scales and Strain Localization Govern the Mechanical Performance of Multi-layer Graphene Assemblies

Wenjie Xia, Luis Ruiz, Nicola M. Pugno and Sinan Keten*

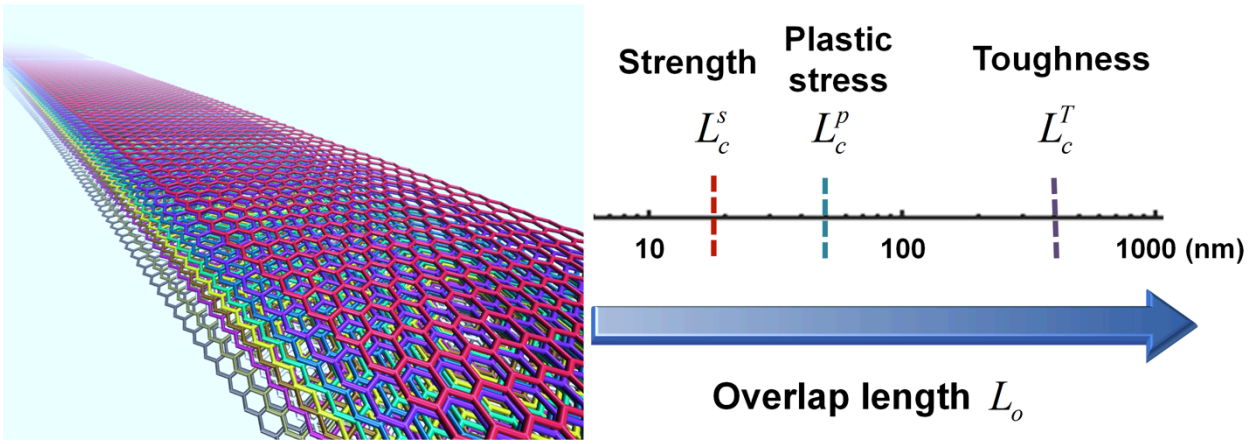

Three critical length scales govern the deformation mechanisms and constitutive response of multilayer graphene.